conceivably enter the lattice and influence the solid's emissive properties.

The other transition metals employed, Cu^{2+} and Ag^+, proved to be efficient quenchers, as they were in solution.[35] In principle, both could quench by electron transfer (eq 6), since the excited uranyl ion should be an extremely strong oxidizing agent ($E°$ for $UO_2^{2+*}/UO_2^+ \simeq 2.60$ V vs. NHE;[35] $E°$ for $Ag^{2+}/Ag^+ \simeq 1.98$ V vs. NHE;[36] $E°$ for Cu^{3+}/Cu^{2+} has been estimated as $\gtrsim 1.8$ V vs. NHE[36]). While this seems like a plausible mechanism for Ag^+, we feel that energy transfer (eq 5) is more likely for Cu^{2+}, since it does possess low-lying excited states (Figure 3). If electron transfer does occur, the back-reaction to generate UO_2^{2+} is energetically very favorable ($E°$ for $UO_2^{2+}/UO_2^+ = 0.06$ V vs. NHE[35]) and would be expected to regenerate the original species. We, in fact, saw no change in sample appearance over hour-long irradiation periods.

The other derivatives examined, NH_4^+, pyH^+, n-$BuNH_3^+$, and n-$OctNH_3^+$, ranged from highly emissive to nonemissive. Both the NH_4^+ and pyH^+ derivatives exhibited little quenching relative to HUP, presumably for the reasons invoked for the closed-shell ions. On the other hand, at room temperature, n-$BuNH_3UP$ exhibited emission that was weaker by ~ 2 orders of magnitude and emission from n-$OctNH_3UP$ could not be detected. Mechanistically, since neither amine has a low-lying excited state, we suspect that quenching proceeds by a photoredox reaction, perhaps analogous to that reported for alcohols in solution (eq 7).[25,37] Such reactions are mechanistically complex. We are presently preparing related amine derivatives of HUP and conducting long- and short-term photolysis experiments to elucidate the quenching mechanism. It is worth noting that at 77 K both the n-$BuNH_3^+$ and n-$OctNH_3^+$ derivatives emit brightly with long lifetimes (Table I). One possible explanation for this low-temperature behavior may be the cessation of a photoreaction such as that described above, perhaps owing to the introduction of steric constraints.

$$UO_2^{2+} + RCH_2OH \rightarrow UO_2^+ + R\dot{C}HOH + H^+ \quad (7)$$

Conclusion

We have shown in this paper that HUP and several of its derivatives prepared by intercalative ion-exchange reactions lend themselves to a systematic examination of excited-state properties. The luminescence exhibited by many of these layered compounds is characteristic of the UO_2^{2+} moiety and serves as a probe of excited-state deactivation processes. Layered compounds in general are receiving considerable attention with regard to intercalation chemistry, yet relatively few studies have examined changes in optical properties accompanying intercalation.[38] The correlations established in this paper suggest that, for suitable hosts, changes in chemical composition accompanying such reactions can be profitably examined by changes in electronic absorption and emission properties. Studies in progress in our laboratories will apply these spectroscopic probes to a broader range of HUP derivatives and reactions.

Acknowledgment. This work was generously supported by the National Science Foundation (Grant CHE-7911218). A.B.E. acknowledges support as an Alfred P. Sloan Fellow (1981-1983). We thank Prof. L. F. Dahl for helpful discussions.

Registry No. HUP, 18433-48-2; NH_4UP, 12161-21-6; pyHUP, 62392-62-5; n-$BuNH_3UP$, 87481-58-1; n-$OctNH_3UP$, 87481-59-2; KUP, 12026-79-8; AgUP, 12244-18-7; $Ca_{0.5}UP$, 68197-84-2; $Zn_{0.5}UP$, 73370-48-6; $Cu_{0.5}UP$, 87462-90-6.

(36) Latimer, W. M. "The Oxidation States of the Elements and Their Potentials in Aqueous Solution", 2nd ed.; Prentice-Hall: New York, 1952; Chapter 11.
(37) Balzani, V.; Carassiti, V. "Photochemistry of Coordination Compounds"; Academic Press: New York, 1970; Chapter 15.
(38) Clement, R. *J. Am. Chem. Soc.* **1981**, *103*, 6998.

Contribution from the Department of Chemistry, University of South Carolina, Columbia, South Carolina 29208

Spectra and Structure of Organophosphorus Compounds. 22.† Microwave, Infrared, and Raman Spectra, Structure, Vibrational Assignment, and Normal-Coordinate Analysis of Methylphosphonothioic Difluoride

J. R. DURIG,* J. A. MEADOWS, Y. S. LI, and A. E. STANLEY

Received October 22, 1982

The microwave spectrum of methylphosphonothioic difluoride, CH_3PSF_2, has been investigated from 18.5 to 39.0 GHz. Both a- and b-type transitions were observed, and R-branch assignments have been made for the ground vibrational state. The rotational constants in the ground vibrational state were found to be $A = 4366.24 \pm 0.03$, $B = 2596.38 \pm 0.01$, and $C = 2496.86 \pm 0.01$ MHz. From a diagnostic least-squares adjustment to fit the rotational constants, the following heavy-atom bond distances were obtained by assuming reasonable structural parameters for the methyl group and skeletal angles: r(P—C) = 1.809 ± 0.004 Å, r(P—F) = 1.547 ± 0.003 Å, and r(P=S) = 1.878 ± 0.003 Å. The infrared (3500–40 cm^{-1}) and Raman (3500–10 cm^{-1}) spectra have been recorded for both the gaseous and solid phases of CH_3PSF_2. Additionally, the Raman spectrum of the liquid was recorded and qualitative depolarization values were obtained. All of the normal modes have been assigned on the basis of infrared band contours, depolarization values, and group frequencies. A normal-coordinate calculation has been carried out by utilizing a modified valence force field to calculate the frequencies and the potential energy distribution. All of these results are compared to similar quantities in some corresponding molecules.

Introduction

Although we have recently carried out a number of spectroscopic studies of compounds containing the difluorophosphine (PF_2) moiety, notably HPF_2,[1] CH_3POF_2,[2,3] PF_2CN,[4] CH_3PF_2,[5] $CH_3CH_2PF_2$,[6] and $(CH_3)_2CHPF_2$,[7] very few compounds with the phosphorus lone pair coordinated with a sulfur

† For paper 21 in this series, see: J. R. Durig, A. E. Stanley, and Y. S. Li, *J. Mol. Struct.*, **78**, 247 (1982).

(1) J. R. Durig, A. J. Zozulin, J. D. Odom, and B. J. Streusand, *J. Raman Spectrosc.*, **8**, 259 (1979).
(2) J. R. Durig, K. S. Kalasinsky, and V. F. Kalasinsky, *J. Mol. Struct.*, **34**, 9 (1976).
(3) J. R. Durig, A. E. Stanley, and Y. S. Li, *J. Mol. Struct.*, **78**, 247 (1982).

0020-1669/83/1322-4134$01.50/0

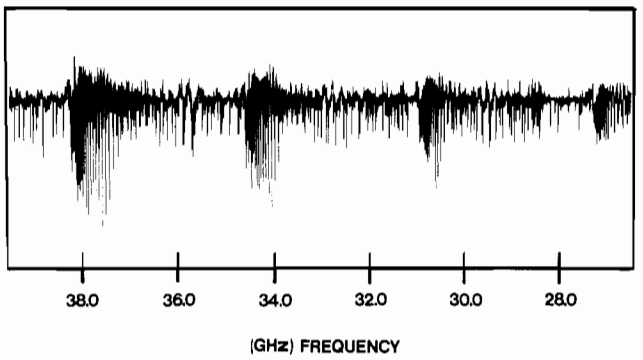

Figure 1. Microwave spectrum of CH_3PSF_2.

atom of the form $RPSF_2$ (R = alkyl) have been studied spectroscopically. However, spectroscopic studies of closely related compounds have been reported: $HPSF_2$,[8] SPF_3,[9] $SPClF_2$,[9] $SPCl_2F$,[9] CH_3OPSF_2,[10] $CH_3OPSClF$,[11] and CH_3PSCl_2.[12] The present study of CH_3PSF_2 will be the first microwave and extensive vibrational study of a compound with the alkyl group directly attached to the thioxodifluorophosphorane (PSF_2) moiety. Infrared data on CH_3PSF_2 have been reported along with two preparations.[13,14] Additionally, an infrared and Raman study[15] of the liquid, including normal coordinates from a simplified valence force field, has been reported. However, these studies contain conflicting spectral data. A detailed vibrational analysis utilizing a pure sample and including a normal-coordinate analysis should clarify the discrepancies.

Compounds containing –P=S bonds have long been of interest due to the contrasting chemical and physical properties of analogous P=O- and P=S-containing compounds. These differences are normally interpreted on the basis of π character and polar bond character of P=S vs. P=O as demonstrated in the ab initio SCF–LCAO–MO study[16] of OPF_3 and SPF_3. These differences are reflected in the chemical characteristics and force constants for these two molecules. Since spectroscopic and theoretical studies of the related compounds CH_3POF_2[2,3,17] and CH_3PF_2[5,17,18] have been reported, it was hoped that a complete rotational and vibrational investigation including normal-coordinate calculations of methylphosphonothioic difluoride would provide insight into trends of fundamental frequencies, barriers to internal rotation, and structural parameters for these compounds as well as some related molecules. The results of such a study are reported herein.

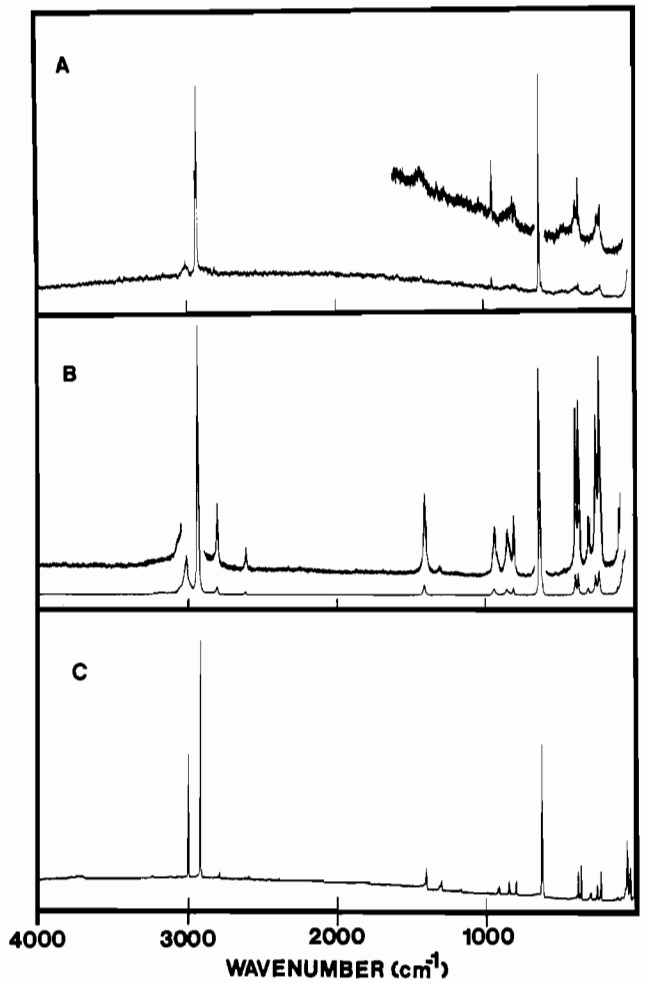

Figure 2. Raman spectra of CH_3PSF_2: (A) gas; (B) liquid; (C) solid.

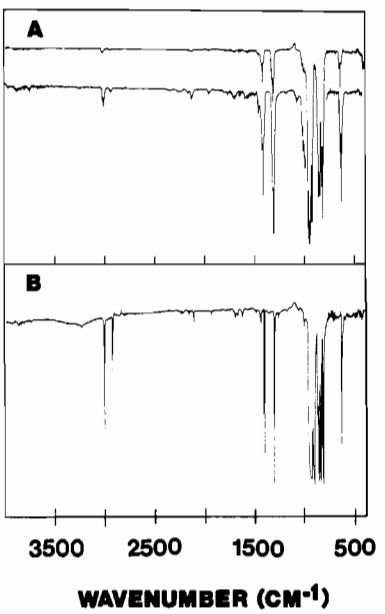

Figure 3. Mid-infrared spectra of CH_3PSF_2: (A) gas; (B) solid.

Experimental Section

The sample of methylphosphonothioic difluoride (CH_3PSF_2) was prepared by the reaction of methylphosphonothioic dichloride (Organometallics) with antimony trifluoride.[19] All sample handling and

(4) A. W. Cox, Jr., A. J. Zozulin, J. D. Odom, and J. R. Durig, *Inorg. Chem.*, **16**, 2049 (1977).
(5) J. R. Durig, A. E. Stanley, and M. R. Jalilian, *J. Raman Spectrosc.*, **10**, 44 (1981).
(6) J. R. Durig, B. J. Streusand, J. S. Church, and Y. S. Li, submitted for publication in *J. Chem. Phys.*
(7) A. E. Stanley, Ph.D. Thesis, University of South Carolina, May 1982.
(8) C. R. Nave and J. Sheridan, *J. Mol. Struct.*, **15**, 391 (1973).
(9) J. R. Durig and J. W. Clark, *J. Chem. Phys.*, **46**, 3057 (1967).
(10) J. R. Durig and J. W. Clark, *J. Chem. Phys.*, **50**, 107 (1969).
(11) J. R. Durig and J. W. Clark, *J. Cryst. Mol. Struct.*, **1**, 43 (1971).
(12) J. R. Durig, F. Block, and I. W. Levin, *Spectrochim. Acta*, **21**, 1105 (1965).
(13) H. L. Boter and A. J. J. Ooms, *Recl. Trans. Chim. Pays-Bas*, **85**, 21 (1966).
(14) R. W. Roesky, *Chem. Ber.*, **101**, 3679 (1968).
(15) V. D. Köttgen, H. Stoll, R. Pantzer, A. Lentz, and J. Goubeau, *Z. Anorg. Allg. Chem.*, **389**, 269 (1972).
(16) A. Serafini and J. F. La Barre, *Chem. Phys. Lett.*, **27**, 430 (1974).
(17) S. von Carlowitz, W. Zeil, P. Pulay, and J. E. Boggs, *J. Mol. Struct. Theochem.*, **87**, 113 (1982).
(18) E. G. Codding, R. A. Creswell, and R. H. Schwendeman, *Inorg. Chem.*, **13**, 856 (1974).
(19) G. I. Drozd, S. Z. Ivin, V. V. Scheluchenko, B. I. Tetel'baum, G. M. Luganski, and A. D. Varshavski, *Zh. Obshch. Khim.*, **37**, 1343 (1967).

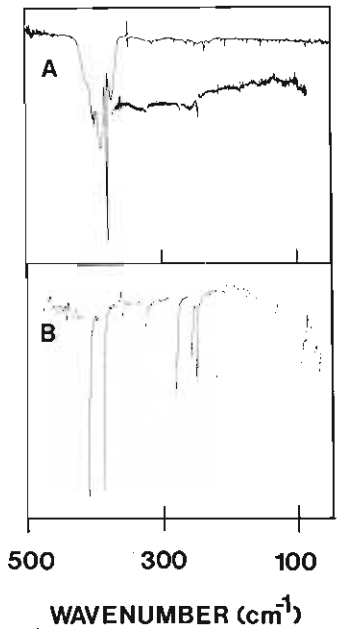

Figure 4. Far-infrared spectra of CH_3PSF_2: (A) gas; (B) solid.

preparative work were completed in a conventional vacuum system using greaseless stopcocks. Purification was accomplished by using a low-temperature vacuum fractionation column. The purity of CH_3PSF_2 was monitored by a comparison of the mid-infrared spectrum of the gas to previously published data.[13-15]

Microwave spectra were recorded on a Hewlett-Packard Model 8460A MRR spectrometer with a Stark cell modulation frequency of 33.3 kHz. All frequencies were measured with the sample held slightly above the temperature of dry ice (~213 K) and are expected to be accurate to within 0.05 MHz. A representative portion of the microwave spectrum is shown in Figure 1.

Raman spectra, as shown in Figure 2, were recorded on a Cary Model 82 spectrophotometer equipped with a Spectra-Physics Model 171 argon ion laser operating on the 514.5-nm line. The laser power used while the liquid or solid phase was being studied was between 0.25 and 0.5 W at the sample. A maximum of 1.5 W at the sample was used for the study of the gas phase. The instrument was calibrated with mercury lines or the plasma lines of the laser. The spectrum of the gas phase was obtained by using the Cary multipass accessory with a sample pressure equal to the maximum vapor pressure at room temperature. The spectrum of the liquid phase was obtained with the sample sealed in a glass capillary held in a standard Cary accessory. The spectrum of the solid phase was obtained by condensing the sample onto a copper block in a typical cold cell[20] cooled by boiling liquid nitrogen. Solid samples were annealed until no further changes were observed in the spectra. Depolarization measurements were made with the standard Cary accessories.

Mid-infrared spectra were recorded from 3500 to 400 cm^{-1} on a Digilab Model FTS-14C Fourier transform infrared interferometer; typical spectra are shown in Figure 3. A Ge/KBr beam splitter, Globar light source, and TGS detector were utilized. The spectrum of the gas phase was obtained with use of a 10-cm cell with CsI windows and a sample pressure of approximately 40 torr. The spectrum of the solid phase was collected by condensing and annealing the sample in a typical cold cell,[20] with outer windows and sample substrate fashioned from CsI, cooled by boiling liquid nitrogen. The instrument was continuously purged with dry nitrogen. Spectra collected on the Digilab Model FTS-14C were obtained by recording the interferograms of the sample and reference cell 100 times at a resolution of 2 cm^{-1}, averaging, and transforming by use of a boxcar apodization function.

Far-infrared spectra were recorded from 600 to 40 cm^{-1} on a Digilab Model FTS-15B Fourier-transform interferometer equipped with a 6.25-μm Mylar beam splitter and a high-pressure Hg arc lamp source. Atmospheric water vapor was removed from the spectrometer housing by continuous purging with dry nitrogen. Typical far-infrared spectra are shown in Figure 4. Spectra of the gas phase were obtained with use of either a 12-cm or 1-m cell equipped with polyethylene windows. The full vapor pressure of the sample at room temperature was used. Interferograms for both the reference and sample cell were recorded 2500 times, averaged, and transformed by use of a boxcar apodization. The spectrum for the solid was obtained with use of a cold cell with a silicon plate as a sample substrate and polyethylene windows. The sample was condensed onto the silicon plate, which was cooled by boiling liquid nitrogen, and annealed until no further spectral changes were noted. The resolution utilized for the spectra of the gas phase was 1.0 or 0.25 cm^{-1}; the resolution used for the solid was 2.0 cm^{-1}.

Frequencies for the Raman spectra are accurate to ±2 cm^{-1} for sharp resolvable bands. Spectra recorded on the Digilab FTS-14C or 15B should have frequencies that are as accurate as the resolution utilized for recording the spectra.

Table I. Rotational Transitions (MHz) of CH_3PSF_2 in the Ground Vibrational State

transition	ν(obsd)	$\Delta\nu^a$
a-type		
$6_{16} \leftarrow 5_{15}$	30 231.15	0.13
$6_{06} \leftarrow 5_{05}$	30 423.70	0.10
$6_{25} \leftarrow 5_{24}$	30 541.11	0.05
$6_{34} \leftarrow 5_{33}$	30 579.06	0.04
$6_{33} \leftarrow 5_{32}$	30 584.63	−0.20
$6_{24} \leftarrow 5_{23}$	30 676.81	0.03
$6_{15} \leftarrow 5_{14}$	30 822.39	0.06
$7_{17} \leftarrow 6_{16}$	35 257.09	0.07
$7_{07} \leftarrow 6_{06}$	35 443.65	−0.03
$7_{26} \leftarrow 6_{25}$	35 620.92	−0.08
$7_{35} \leftarrow 6_{34}$	35 680.15	−0.12
$7_{34} \leftarrow 6_{33}$	35 693.08	−0.19
$7_{25} \leftarrow 6_{24}$	35 829.61	−0.08
$7_{16} \leftarrow 6_{15}$	35 940.64	−0.04
b-type		
$4_{14} \leftarrow 3_{03}$	21 705.09	0.14
$5_{15} \leftarrow 4_{04}$	26 573.18	0.19
$6_{06} \leftarrow 5_{15}$	29 237.21	0.03
$5_{24} \leftarrow 4_{13}$	30 426.05	−0.23
$6_{16} \leftarrow 5_{05}$	31 417.62	0.17
$6_{25} \leftarrow 5_{14}$	35 271.22	−0.13
$6_{24} \leftarrow 5_{15}$	37 037.5	0.21

[a] ν(obsd) − ν(calcd); calculated from rotational constants listed in Table II.

Microwave Spectra

On the basis of the molecular structural parameters of CH_3POF_2[3] and CH_3PF_2,[18] as well as those of $SPHF_2$[8] and SPF_3,[21] the calculations indicate that the CH_3PSF_2 molecule has its plane of symmetry formed by the *a* and *b* inertial axes with the *c* axis perpendicular to the plane of symmetry and has a κ value of −0.90. The low-resolution microwave spectrum of CH_3PSF_2 showing the complexity of the absorption is shown in Figure 1. On the basis of the initially assumed structure, the dipole of the molecule should lie between the *a* and *b* inertial axes and therefore both a- and b-type transitions are expected.

Initial surveys of the spectra showed no clearly recognizable a-type bands. However, it is clear that there are band heads of b-type Q-branches present in the spectrum and separated by about 3750 MHz. The predicted separation between the b-type Q-branch band heads should be $A - {}^1/_2(B + C)$, and the structural parameters were adjusted until the calculated separation agreed to within 25 MHz of the observed separation. These rotational constants were then utilized with the rigid-rotor model to predict both a- and b-type R-branches. The initial assignment of the individual rotational lines was made for the a-type R-branch series $(J + 1)_{1,J+1} \leftarrow J_{1,J}$, $(J + 1)_{0,J+1} \leftarrow J_{0,J}$, and $(J + 1)_{1,J} \leftarrow J_{1,J-1}$ where $J = 5$ and 6.

(20) J. R. Durig, S. F. Bush, and F. G. Baglin, *J. Chem. Phys.*, **49**, 2106 (1968).

(21) K. Karakida and K. Kuchitsu, *Inorg. Chim. Acta*, **16**, 29 (1976).

Table II. Ground Vibrational State Rotational Constants (MHz) and Moments of Inertia (u·Å²)[a] of CH_3PSF_2

A	4366.24 ± 0.03
B	2596.38 ± 0.01
C	2496.86 ± 0.01
κ	−0.89
I_a	115.75
I_b	194.65
I_c	202.41

[a] Conversion factor 505 391 MHz·Å².

Table III. Diagnostic Least-Squares Adjustment of the Structural Parameters of CH_3PSF_2

parameter	initial value	estimated uncertainty	adjusted value
r(PC), Å	1.810	±0.020	1.809 ± 0.004
r(PF), Å	1.540	±0.020	1.547 ± 0.003
r(PS), Å	1.870	±0.020	1.878 ± 0.003
∠SPC, deg	116.0	fixed	
∠FPF, deg	98.8	fixed	
∠FPC, deg	101.3	fixed	

rotational const	obsd	calcd	Δ
A	4366.24	4366.24	0.0
B	2596.37	2596.37	0.0
C	2496.86	2496.86	0.0

From these assignments the b-type R-branches were predicted and measured. Other lines were then measured, and the assignment was confirmed by checking the qualitative Stark effect as well as the fit with the rigid-rotor model. The measured transitions of CH_3PSF_2 for the ground vibrational state are listed in Table I, and the rotational constants calculated from these observed transitions are listed in Table II.

Although the individual Q-branches were not measured, frequencies based upon the rotational constants from the measured a- and b-type R-branches were in reasonable agreement with the observed lines for the higher J Q-branches when one took into account the expected centrifugal distortion. The lower J Q-branches were too weak to be measured accurately or were masked by other transitions. No splitting of the lines due to the methyl rotation was observed, and attempts to measure the dipole moment failed because clear Stark lobes, which can be followed at reasonable voltages for measuring the dipole moments, could not be found.

Molecular Structure. Of major interest in this study was the determination of the structural parameters associated with the phosphonothioic difluoride moiety, but a complete determination of the structural parameters is not possible from only three rotational constants. However, limiting values for the heavy-atom skeletal parameters can be obtained by assuming tetrahedral angles for the methyl group and C–H bond distances of 1.085 Å and by extrapolating starting values for the bond distances of the $CPSF_2$ moiety from the molecules SPF_3,[21] CH_3PF_2,[18] and CH_3POF_2.[3] The initial values and uncertainties utilized are very similar to those used in the study of CH_3POF_2[3] except for the P=S bond distance, which was taken from SPF_3[21] with a predicted elongation of 0.01 Å due to substitution of a methyl group for a fluorine atom. With use of the diagnostic least-squares method of Curl[22] and a program obtained from Wells and Malloy,[23] the three bond distances were fit to the experimental rotational constants. The initially assumed structural parameters, estimated uncertainties, and adjusted values are reported in Table III. The listed uncertainties are the statistical uncertainties and do not reflect the uncertainties in the bond angles, but small changes in these parameters (such as 1°) did not significantly change the results.

Vibrational Assignment

On the basis of C_s symmetry, the 18 fundamentals of CH_3PSF_2 will be distributed as 11 A′ + 7 A″, with all frequencies being both Raman and infrared active. The A′ modes will give rise to polarized Raman lines and A, B, or A/B hybrid infrared band contours (P–R separations of 16 cm^{-1}) whereas the A″ modes should yield depolarized Raman lines and C-type infrared band contours with P–R separations of 20 cm^{-1}. In actuality, pronounced Q-branches were frequently observed for both the A/B hybrid and C-type bands, but the utilization of the depolarization ratios clearly defined the A″ modes and shows reasonable correspondence with the C-type bands observed in the infrared spectrum of the gas phase. Therefore, the proposed assignment of the normal modes is based on the infrared band contours, the depolarization values, and the group frequencies.[8-12,24,25]

Carbon–Hydrogen Modes. The carbon–hydrogen stretching modes can be readily assigned at 3018 (A′ and A″) and 2942 cm^{-1} (A′), with the lower frequency band corresponding to the symmetric CH_3 stretch. Even in the spectra of the solid, there is little indication of the two components of the antisymmetric stretch. The CH_3 antisymmetric deformations are assigned at 1418 cm^{-1}, but in this case both components are clearly observed in the infrared spectrum of the solid. The CH_3 symmetric deformation gives rise to the strong type-A band at 1314 cm^{-1}, but the corresponding polarized Raman line is unusually weak. The assignment of the two CH_3 rocking modes is not as straightforward because there are four bands in the region from 960 to 840 cm^{-1}, where they are expected. We have taken the 848- and 859-cm^{-1} bands as the out-of-plane and in-plane CH_3 rocks, respectively, because the two higher frequency bands are more consistently assigned as the phosphorus–fluorine stretching modes.

Skeletal Vibrations. The heavy atoms will contribute nine fundamentals (6 A′ + 3 A″), four of which are stretching modes and the remaining five bending modes. The PF_2 symmetric and antisymmetric stretches are assigned at 956 and 926 cm^{-1}, respectively, where both the depolarization values and band contours are consistent with the assignment. It should be pointed out that the these frequencies are within 10 cm^{-1} of the corresponding modes in $SPClF_2$,[9] where coupling with the CH_3 rocks is not possible, as well as with those in CH_3OPSF_2,[10] where the CH_3 rocks are at 1188 cm^{-1}, and that no mixing was found with deuteration. The PF_2 stretching modes for these phosphorus(V) molecules appear to be good group frequencies even though the normal-coordinate calculations indicate considerable mixing with the other normal modes. The other two stretches, the P—C and P=S, are assigned at 820 and 644 cm^{-1}, respectively, where appreciable mixing is expected since the P=S mode is about 50 cm^{-1} lower than the corresponding mode in $SPHF_2$[8] and SPF_3.[9]

The five bending motions can be described as the PF_2 wag, deformation, and twist along with the in- and out-of-plane CPS bends. The PF_2 bends are assigned at 399, 381, and 311 cm^{-1}, with the highest frequency being the deformation and the lowest the twist. Although the two CPS bends are degenerate at 262 cm^{-1} in the CH_3PSCl_2 molecule,[12] the out-of-plane mode can be clearly identified at 261 cm^{-1} as a C-type band with a corresponding depolarized Raman line. The CPS in-plane mode is assigned to the A-type band at 234 cm^{-1}, where the corresponding Raman line in the spectrum of the gas is clearly polarized.

(22) R. F. Curl, Jr., *J. Comput. Phys.*, **6**, 367 (1970).
(23) J. A. Wells and T. B. Malloy, Jr., *J. Chem. Phys.*, **60**, 2132 (1974).
(24) J. R. Durig, B. R. Mitchell, J. S. DiYorio, and F. Block, *J. Phys. Chem.*, **70**, 3190 (1966).
(25) J. R. Durig and J. M. Casper, *J. Phys., Chem.*, **75**, 1956 (1971).

Table IV. Observed[a] Infrared and Raman Frequencies (cm^{-1}) and Vibrational Assignment of CH_3PSF_2

infrared				Raman						assignt	
gas	rel int	solid	rel int	gas	rel int	liquid	rel int	solid	rel int	ν_i	approx description
		3250	vvw, br							$\nu_2 + \nu_{16}$	
						3168	vw, br			$\nu_2 + \nu_{18}$	
3024 R		3006	sh								
3018 Q	w	3003	m	3015	w, dp	3005	w, dp	3004	m	ν_1, ν_{12}	CH_3 antisym str
3010 P											
				2947	sh						
2942 Q	vw	2926	m	2942	s, p	2927	s, p	2926	s	ν_2	CH_3 sym str
				2887	vw, p						
				2863	vw, p	2854	m, p	2851	w		
						2800	w, p			$2\nu_{13}$	
		2791	vw					2795	vw	$\nu_4 + \nu_{13}$	
						2687	w, p				
		2661	w								
						2633	w, p				
		2614	vw, p			2608	w, p	2603	vw		
1425 Q?											
1418 Q	w	1418	m	1420	vw, br	1410	w, dp	1420	sh, vw	ν_3, ν_{13}	CH_3 antisym def
1408 P		1404	s					1410	w		
1323 R											
1314 Q, A	s	1308	vs	1310	vw, br	1310	vw, p	1306	vw	ν_4	CH_3 sym def
1307 P											
963 R											
956 Q	vs	940	vs	957	w, p	944	w, p	946	vw, br	ν_5	PF_2 sym str
947 P											
								929	vw		
926 Q, C	s	906	vs			925	w, dp	920	vw	ν_{14}	PF_2 antisym str
		876	m								
859 Q	s	860	vs	860	vw, br	859	w, p	856	w	ν_6	CH_3 rock
848 Q	s	842	s	852	vw, br	842	vvw, dp	848	vw	ν_{15}	CH_3 rock
827 R											
820 Q, A	s	820	vs	820	vvw, p	814	w, p	809	vw	ν_7	PC str
812 P											
650 R											
644 Q, A	w	634	s	643	s, p	640	s, p	635	m	ν_8	PS str
635 P		630	sh								
408 R											
401 Q	m										
399 ctr		398	m	400	w, p	400	w, p	396	w	ν_9	PF_2 def
398 Q											
389 R											
381 Q	m	377	m	381	w, p	380	w, p	375	w	ν_{10}	PF_2 wag
373 P											
321 R											
311 Q, C	w	314	vw	311	vw	312	w, dp	312	vw	ν_{16}	PF_2 twist
301 P											
263 Q											
261 Q, C	w	269	w	261	vw, dp, ctr	265	w, dp	269	w	ν_{17}	CPS out-of-plane bend
		245	vw	243	vw, dp					ν_{18}	CH_3 torsion
245 R											
234 Q, A	w	238	w	236	w, p	240	w, dp	242	m	ν_{11}	CPS in-plane bend
225 P											
		97	vw								two phonon bands
		91	vw								
		85	vw								
84	vw										
		81	vw								lattice modes
		76	w								
								66	m		
		56	vw								
								47	w		

[a] Abbreviations used: br, broad; sh, shoulder; dp, depolarized; p, polarized; v, very; s, strong; m, medium; w, weak; A, B, A/B, and C refer to infrared gas-phase band contours; ctr, center of B-type band.

Internal Rotation. The only mode remaining to be assigned is the CH_3 torsion. In the Raman effect, a broad, depolarized band in the gas phase appears centered at 243 cm^{-1}. While there is no counterpart in the far-infrared spectrum of the gas, a band does appear in the far-infrared spectrum of the solid at 245 cm^{-1} which may correspond to this band or be due to factor group splitting of the in-plane CPS bend. The Raman spectrum of the gas phase was scanned a number of times in attempts to observe "hot bands" or "overtones" of this torsion. Two "hot bands" were observed at 231 and 217 cm^{-1} which could belong to the torsion or to the CPS in-plane bend that occurs at 236 cm^{-1}. From the frequency of 243 cm^{-1} for ν_{18} and the potential energy function for a threefold torsional oscillation that can be written as $V(\alpha) = (V_3/2)(1 - \cos 3\alpha) + (V_6/2)(1 - \cos 6\alpha)$, a value for V_3, the barrier to internal rotation, of 1340 ± 10 cm^{-1} (3.83 kcal/mol) was obtained. The reduced moment of inertia constant, $F = (h/8\pi^2 c I_r)$, where I_r is the reduced moment of inertia for the internal rotation, utilized in this calculation has a value of 5.430 cm^{-1}. Although this potential function predicted the first "hot band"

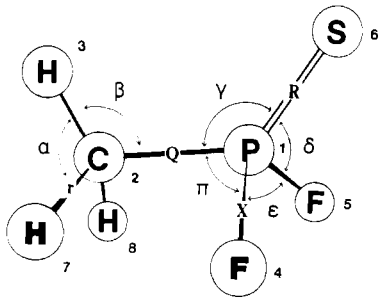

Figure 5. Internal coordinates for CH_3PSF_2.

Table V. Symmetry Coordinates for CH_3PSF_2

species (C_s)	symmetry coordinate	description
A′	$S_1 = 2r_3 - r_7 - r_8$	CH_3 antisym str
	$S_2 = r_3 + r_7 + r_8$	CH_3 sym str
	$S_3 = 2\alpha_3 - \alpha_7 - \alpha_8$	CH_3 antisym def
	$S_4 = \alpha_3 + \alpha_7 + \alpha_8 - \beta_3 - \beta_7 - \beta_8$	CH_3 sym def
	$S_5 = X_4 + X_5$	PF_2 sym str
	$S_6 = 2\beta_3 - \beta_7 - \beta_8$	CH_3 in-plane rock
	$S_7 = Q$	PC str
	$S_8 = R$	PS str
	$S_9 = \pi_4 + \pi_5 - \delta_4 - \delta_5$	PF_2 wag
	$S_{10} = 4.45\epsilon - 0.45\gamma - \pi_4 - \pi_5 - \delta_4 - \delta_5$	PF_2 def
	$S_{11} = 0.45\epsilon - 4.45\gamma + \delta_4 + \delta_5 + \pi_4 + \pi_5$	CPS in-plane bend
	$S_{12} = \alpha_3 + \alpha_7 + \alpha_8 + \beta_3 + \beta_7 + \beta_8$	CH_3 redundancy
	$S_{13} = \gamma + \delta_4 + \delta_5 + \pi_4 + \pi_5 + \epsilon$	PSF_2 redundancy
A″	$S_{14} = r_7 - r_8$	CH_3 antisym str
	$S_{15} = \alpha_7 - \alpha_8$	CH_3 antisym def
	$S_{16} = X_4 - X_5$	PF_2 antisym str
	$S_{17} = \beta_7 - \beta_8$	CH_3 out-of-plane rock
	$S_{18} = \pi_4 - \pi_5 - \delta_4 + \delta_5$	PF_2 twist
	$S_{19} = \pi_4 - \pi_5 + \delta_4 - \delta_5$	CPS out-of-plane bend
	$S_{20} = \tau$	CH_3 torsion

at 229.0 cm^{-1} and the second at 213.6 cm^{-1}, which is in reasonable agreement with the observed lines, the V_6 term was neglected in the barrier calculation due to lack of assurance that the observed bands belonged to the torsion.

The complete vibrational assignment is tabulated in Table IV, where idealized descriptions are given for the normal modes. Only a limited number of overtone or combination bands were observed, but possible assignments for them are also presented in Table IV. The number of observed lattice modes in the infrared spectrum is consistent with two or four molecules per primitive cell, but the limited number of observed Raman lines in the lattice region is somewhat surprising and supports only two molecules per primitive cell.

Normal-Coordinate Calculation

In the order to obtain a more complete interpretation of the vibrational spectrum of CH_3PSF_2 and to determine the degree of mixing of those fundamentals occurring at intermediate and low frequencies, especially the P═S and P—C fundamentals, normal-coordinate calculations were undertaken. The analysis was made by utilizing the Wilson GF-matrix method[26] and the programs written by Schachtschneider.[27] The G matrix was calculated from the structural parameters determined in the microwave study reported herein. Initial force constants for the P—F, P—C, and P═S stretches were taken from the published values for CH_3PSF_2 by Köttgen et al.,[15] and the initial values for the FPF, HCP, and FPC bends were taken from those of CH_3PF_2.[5] Initial force constants for the methyl group were taken from the reported values from the work of Snyder and Schachtschneider.[28] The 18 internal coordinates consisting of the bond lengths and bond angles shown in Figure 5 were used in the first step of the calculations, and symmetrization was accomplished by using the symmetry coordinates listed in Table V. The S_{12} and S_{13} symmetry coordinates were defined as zero-coordinate redundancies. The force constants utilized in this modified valence force field are given in Table VI, and the calculated frequencies and associated normalized potential energy distribution are listed in Table VII. The average difference between the observed and calculated frequencies was found to be 5.0 cm^{-1} (0.9%).

In general, the force constants associated with the CH_3 stretch and CH_3 deformation are in good agreement with those reported by Snyder and Schachtschneider[28] for hydrocarbons. The spectral region containing the CH_3 rock, the PF_2 stretches, the PS stretch, and the PC stretch merits some discussion. During the iteration of the force constants it was found that considerable mixing among these modes was present, and great care had to be taken to avoid reversing the proposed assignments. Despite this mixing, the correct order was followed in the assignment of the PF_2 symmetric stretch and the CH_3

Table VI. Internal Force Constants[a] for CH_3PSF_2

force const	description	value,[b] mdyn/Å
K_r	C–H str	4.89
K_Q	P–C str	3.63
K_X	P–F str	5.18
K_R	P=S str	5.05
H_α	H–C–H bend	0.51
H_β	H–C–P bend	0.48
H_γ	C–P=S bend	0.58
H_δ	F–P=S bend	0.77
H_ϵ	F–P–F bend	1.57
H_π	C–P–F bend	1.42
F_{rr}	C–H str/C–H str	0.05
F_{XR}	P–F str/P=S str	0.59
F_{QR}	P–C str/P=S str	0.34
F_{XX}	P–F str/P–F str	0.15
$F_{Q\beta}$	P–C str/H–C–P bend	−0.11
$F_{\beta\beta}$	H–C–P bend/H–C–P bend	−0.04
$F_{\pi\pi}$	F–P–C bend/F–P–C bend	0.29

[a] Valence force field constants. [b] Bending coordinates are weighted by 1 Å.

Table VII. Observed[a] and Calculated Frequencies (cm^{-1}) and Potential Energy Distribution[b] (PED) for the Normal Modes of CH_3PSF_2

vib no.	obsd	calcd	assignt and PED
A′ ν_1	3018	3018	100% CH_3 antisym str
ν_2	2942	2942	100% CH_3 sym str
ν_3	1418	1420	95% CH_3 antisym def
ν_4	1314	1312	87% CH_3 sym def, 12% PC str
ν_5	956	959	35% PF_2 str, 35% CH_3 rock, 17% PS str
ν_6	859	857	42% CH_3 rock, 29% PF_2 str, 19% PC str
ν_7	820	816	29% PC str, 28% PS str, 25% PF_2 str, 9% PF_2 wag
ν_8	644	648	38% PS str, 36% PC str, 18% CH_3 rock
ν_9	399	402	66% PF_2 def, 26% PF_2 wag
ν_{10}	381	381	43% PF_2 wag, 26% PF_2 def, 21% PS str
ν_{11}	234	235	83% CPS in-plane bend, 15% PF_2 wag
A″ ν_{12}	3018	3018	100% CH_3 antisym str
ν_{13}	1418	1419	95% CH_3 antisym def
ν_{14}	926	930	48% PF_2 str, 47% CH_3 out-of-plane rock
ν_{15}	848	842	48% CH_3 out-of-plane rock, 48% PF_2 str
ν_{16}	311	311	64% PF_2 twist, 33% CPS out-of-plane bend
ν_{17}	261	260	58% CPS out-of-plane bend, 40% PF_2 twist

[a] All frequencies are infrared gas frequencies. [b] Contributions of less than 5% are not included.

(26) E. B. Wilson, J. C. Decius, and P. C. Cross, "Molecular Vibrations", McGraw-Hill, New York, 1955.
(27) J. H. Schachtschneider, Technical Reports 231-64 and 57-65, Shell Development Co., Emeryville, CA, 1964, 1965.
(28) R. G. Snyder and J. H. Schachtschneider, *Spectrochim. Acta*, **21**, 169 (1965).

Table VIII. Structural Parameters for Molecules Similar to CH_3PSF_2

parameter	molecule									
	PF_3	OPF_3	SPF_3	CH_3PF_2	CH_3POF_2	CH_3PSF_2	$HPSF_2$	$(CH_3)_3P$	$(CH_3)_3PO$	$(CH_3)_3PS$
r(PF), Å	1.5700 ± 0.0012	1.524 ± 0.003	1.538 ± 0.003	1.587 ± 0.008	1.544 ± 0.011	1.547 ± 0.003	1.551 ± 0.005			
r(PS), Å			1.866 ± 0.005			1.878 ± 0.003	1.867 ± 0.005			1.940 ± 0.002
r(PO), Å		1.435 ± 0.006			1.442 ± 0.009				1.476 ± 0.002	
r(PC), Å				1.817 ± 0.017	1.795 ± 0.019	1.809 ± 0.004		1.844 ± 0.003	1.809 ± 0.002	1.818 ± 0.002
∠FPF, deg	97.8 ± 0.2	101.3 ± 0.2	99.6 ± 0.3	98.0 ± 0.6	99.2 ± 1.0	98.8	98.6 ± 0.2			
∠FPS, deg			117.9 ± 0.3			118.2	117.4 ± 0.2			
∠FPO, deg		116.8			121.4					
∠FPC, deg				98.0 ± 0.6	100.5 ± 2.3	101.3				
∠SPC, deg						116.0				114.1 ± 0.2
∠OPC, deg					118.2 ± 1.5				114.4 ± 0.7	
∠CPC, deg								98.8		
ref	31	32	21	3, 18	3	this study	8	33	34	34

in-plane rock. Very large contributions from the PF_2 stretch and PS stretch, as well as some mixing of the PF_2 wag, are found for the band assigned as the PC stretch. The band assigned as the PS stretch is found to have nearly equal contributions of the PC and PS stretches and a large amount of the CH_3 rock. In the A″ block the PF_2 antisymmetric stretch and the CH_3 out-of-plane rock are nearly equally mixed. Considerable mixing was also found for the PF_2 wag, deformation, and twist and the CPS bends. The values of the force constants for the bending motions are in reasonable agreement with those reported for the similar force constants in CH_3PF_2,[5] HPF_2,[1,29] and SPF_3,[30] as well as those previously reported[15] for CH_3PSF_2.

Discussion

Since there are considerable structural data available on PF_2, POF_2, and PSF_2 compounds, it is interesting to compare the bond distances obtained for CH_3PSF_2 with the structural parameters of similar molecules. In Table VIII are summarized the structural data for a number of such compounds. It can be seen that the substitution of a CH_3 group for a fluorine atom increases the P–F bond length by 0.017 Å from PF_3[31] to CH_3PF_2,[18] by 0.020 Å from OPF_3[32] to CH_3POF_2,[3] and by 0.009 from SPF_3[21] to CH_3PSF_2. Although the absolute differences in this numbers are probably not meaningful, it appears that there is a clear trend of elongation of the PF distance with methyl substitution. Similarly, there appears to be an increase of the P=O and P=S bond lengths with the substitution of a methyl group for a fluorine atom. The effect is quite dramatic when one considers that the P=S distance in SPF_3 is 1.866 Å but in $(CH_3)_3PS$ it is 1.940 Å and, for the corresponding oxygen containing compounds, the elongation is 0.041 Å. Thus, the P=S distance of 1.878 Å for CH_3PSF_2 is consistent with this trend and appears to be unquestionably due to the substitution of the methyl group since the P=S bond length in $HPSF_2$[8] is within 0.001 Å of the value for the corresponding bond in SPF_3.[21]

The P–C bond distance shows a very large variation when the methyl groups on $(CH_3)_3P$ are replaced by fluorine atoms or when the lone pair is used for bonding as in the oxygen- and sulfur-containing molecules. For example, the P–C distance in $(CH_3)_3P$[33] is 1.844 Å but this same distance is 1.817 Å in CH_3PF_2,[3,18] 1.809 Å in $(CH_3)_3PO$,[34] and 1.795 Å in CH_3POF_2.[3] For the sulfur analogues this distance is 1.818 Å in $(CH_3)_3PS$[34] and 1.809 in CH_3PSF_2 (see Table VIII). Therefore, the P–C distance that we have obtained is very consistent with these trends.

Recently von Carlowitz et al.[17] calculated the structural parameters of CH_3POF_2 and CH_3PF_2 by MO–LCAO–SCF single-determinant calculations using split valence-shell basis sets with polarization functions on phosphorus and predicted P–C bond lengths in these compounds of 1.753 and 1.799 Å, respectively. However, these values appear to be too short, and it appears that such calculations will significantly underestimate the P–C bond length in these type of compounds. Nevertheless, the relative values of a given structural parameter in a series of related molecules should be more accurate than their absolute values. Additionally, it is clear from these results, along with the structural parameters obtained from the microwave studies, that the withdrawal of the electronic charge from the phosphorus atom by coordination with oxygen or sulfur will cause a shrinkage of the bonds between the phosphorus atom and the other electronegative substituents.

Prior to discussing the vibrational assignment of CH_3PSF_2, a few comments on sample purity seem to be in order. Obviously, in the last two decades the ability to purify samples has improved dramatically, and the vibrational data in the literature on this compound[13-15] are indicative of this improvement. The infrared spectrum of CH_3PSF_2 is shown in the paper by Boter and Ooms[13] where the preparation of CH_3PSF_2 by the fluorination of CH_3PSCl_2 using SbF_3 followed by the distillation of CH_3PSF_2 at 61–63 °C was reported. In the paper by Roesky,[14] a different preparation was reported and some extraneous bands in the mid-infrared spectrum were reported. In the study of CH_3PSF_2 by Köttgen et al.,[15] the PC stretch is assigned to a band at 748 cm^{-1}, which does not appear in the spectra we obtained. It is apparent from our study that the spectral data reported by Roesky[14] and Köttgen et al.[15] contained the contaminant CH_3POF_2, a compound whose strongest band in the Raman spectrum is at 759 cm^{-1}. Additionally, at least a second contaminant is present that yields bands at 1266, 1159, 1030, and 804 cm^{-1}. These bands were found to be present in the first sample of

(29) V. D. Dunning and R. C. Taylor, *Spectrochim. Acta, Part A*, **35A**, 479 (1979).
(30) H. F. Shurvell, *Spectrochim. Acta, Part A*, **25A**, 973 (1969).
(31) Y. Morino, K. Kuchitsu, and T. Moritani, *Inorg. Chem.*, **8**, 867 (1969).
(32) T. Moritani, K. Kuchitsu, and Y. Morino, *Inorg. Chem.*, **10**, 344 (1971).
(33) B. Beagley and A. R. Medwid, *J. Mol. Struct.*, **38**, 229 (1977).
(34) C. J. Wilkins, K. Hagen, L. Hedberg, Q. Shen, and K. Hedberg, *J. Am. Chem. Soc.*, **97**, 6352 (1975).

Table IX. Comparison of the Barriers to Internal Rotation of Some Similar Molecules

molecule	barrier, kcal/mol	ref
CH_3PH_2	1.96	36
CH_3PF_2	1.74	5
CH_3PCl_2	3.37	25
CH_3POF_2	3.0 ± 0.2	3
CH_3POCl_2	4.4	25
CH_3PSF_2	3.82	this study
CH_3PSCl_2	3.2	25

CH_3PSF_2 that we prepared but disappeared when the technique of distillation followed by vacuum fractionation was utilized.

The tabulated frequency limits for the infrared absorption characteristic of the P═S stretching mode have varied widely, and it has been concluded that there are two vibrational frequencies with ranges 685–862 cm^{-1} (band I) and 550–730 cm^{-1} (band II) that are associated with the presence of this bond.[35] Although it has been suggested by some authors that the second band could originate from the presence of a second conformer, it is clear from the normal-coordinate calculations that the higher frequency band originates from the mixing of the P—C and P═S stretching modes. Also, it should be pointed out that the relative intensity of the Raman band at 643 cm^{-1} compared to the 820-cm^{-1} band indicates that the lower frequency band is more appropriately described as the phosphorus–sulfur stretch and our force field overascribes the amount of mixing between these two modes. However, it appears that all compounds with the general formula $RPSY_2$, where R is an alkyl group and the Ys are halogens, OR, NR_2, or other alkyl groups, will show such mixing, but the presence of a second conformer can be more easily detected in the Raman effect with the appearance of a second band in the 600-cm^{-1} spectral region.

In the vibrational study of CH_3PF_2,[5] the question arose as to whether the trend in barrier values observed in group 4A compounds of the type CH_3MH_3, CH_3MH_2F, CH_3MHF_2, and CH_3MF_3 would be followed for the corresponding compounds containing a group 5A element. In group 4A, carbon is unique in that substitution of fluorine for hydrogen in ethane results in an initial increase in the barrier to internal rotation followed by a very small decrease in the barrier as substitution of subsequent fluorines follows. Analogous silicon[36] and germanium[37] compounds show a decrease in the barrier to internal rotation as fluorine substitution occurs. Apparently nitrogen is unique in compounds containing group 5A elements because a dramatic increase in the barrier to internal rotation is observed with fluorine substitution whereas for the analogous phosphorus and arsenic compounds a decrease in the barrier is observed with fluorine substitution.[5]

In Table IX are summarized some barriers to internal rotation for molecules similar to CH_3PSF_2. As the barrier changes from CH_3PH_2[38] to CH_3PF_2,[5] one observes an expected decrease from 1.96 to 1.74 kcal/mol, but in CH_3PCl_2[25] a large increase to 3.37 kcal/mol is observed due to the effect of the chlorine substitution. Similarly, the barrier values for CH_3PF_2,[5] CH_3POF_2,[3] and CH_3PSF_2 are found to be 1.74, 3.0, and 3.82 kcal/mol, respectively. In comparing the barriers for CH_3POF_2[3] and CH_3POCl_2,[25] one finds an expected increase from 3.0 to 4.4 kcal/mol. However, from CH_3PSF_2 to CH_3PSCl_2[25] we see a decrease from 3.82 to 3.2 kcal/mol, which does not fit into the expected trend, and it appears that the barrier in CH_3PSCl_2 is too low. Therefore, either the earlier assignment[25] of the weak Raman line at 221 cm^{-1} to the torsional mode of CH_3PSCl_2 is in error or the barrier has a very unusual value. It is possible that this band is a two-phonon band and the torsional mode lies under one of the skeletal bends. Since the barrier value for this molecule appears to be out of line, it would be useful to verify the assignment of the 221-cm^{-1} band with deuterium substitution.

Acknowledgment. We gratefully acknowledge the financial support of this study by the National Science Foundation through Grant CHE-82-15492.

Registry No. CH_3PSF_2, 753-72-0; methylphosphonothioic dichloride, 676-98-2; antimony trifluoride, 7783-56-4.

(35) L. C. Thomas, "Interpretation of the Infrared Spectra of Organophosphorus Compounds", Heyden, London, 1974.
(36) J. R. Durig, Y. S. Li, and C. C. Tong, *J. Mol. Struct.*, **14**, 255 (1972).
(37) L. C. Krisher and J. A. Morrison, *J. Chem. Phys.*, **64**, 3556 (1976).
(38) D. R. Lide, Jr., *J. Chem. Phys.*, **27**, 343 (1957).

Notes

Contribution from the Department of Chemistry, The Ohio State University, Columbus, Ohio 43210

Formation of Diketone Ligands by Oxidation of Macrocyclic Iron(II) Complexes with Molecular Oxygen

Dennis P. Riley† and Daryle H. Busch*

Received January 18, 1983

Previously we have reported that low-spin iron(II) complexes of neutral tetraaza macrocyclic ligands containing secondary amine groups (NHR_2) coordinated to iron(II) react with molecular oxygen producing, via an oxidative dehydrogenation, stable coordinated triene and tetraene ligands.[1,2] In the course of our studies concerning the reactivity of iron(II) complexes **1** and **2** containing bis(β-diimine) macrocyclic ligands,[3,4] we

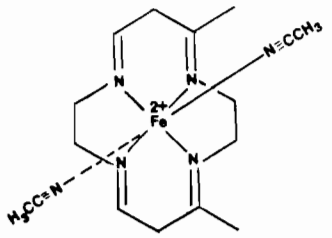

1 **2a**, X = $(CH_2)_2$, Y = $(CH_2)_3$
b, X = $(C(CH_3)_2)_2$, Y = $(CH_2)_3$
c, X = Y = $(CH_2)_3$

discovered that molecular oxygen also reacts with these com-

†Present address: Miami Valley Laboratories, The Procter & Gamble Co., Cincinnati, OH 45247.

(1) Goedken, V. L.; Busch, D. H. *J. Am. Chem. Soc.* **1972**, *94*, 7355.
(2) Dabrowiak, J. C.; Busch, D. H. *Inorg. Chem.* **1975**, *14*, 1881.
(3) Riley, D. P.; Stone, J. A.; Busch, D. H. *J. Am. Chem. Soc.* **1976**, *98*, 1752.

0020-1669/83/1322-4141$01.50/0